RSC Advances

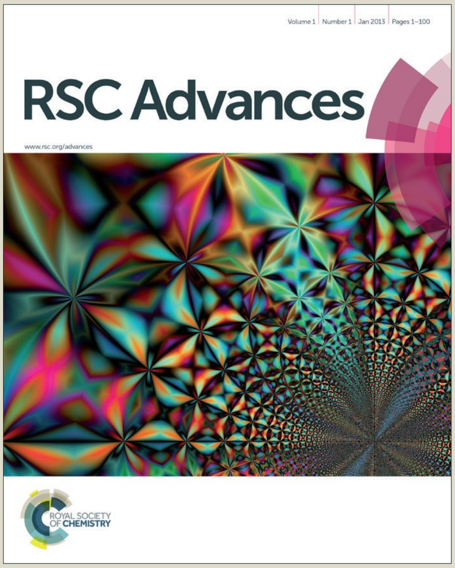

ROYAL SOCIETY OF CHEMISTRY

www.rsc.org/advances

Density Functional Theory Study on Organically Surface-Modified Silicene

Rong Wang,[1,2] *Xiaodong Pi,*[1*] *Zhenyi Ni,*[1] *Yong Liu*[1] *and Deren Yang*[1]

[1]State Key Laboratory of Silicon Materials and School of Materials Science and
Engineering, Zhejiang University, Hangzhou 310027, China
[2] Key Laboratory of Interface Science and Engineering in Advanced Materials,
Ministry of Education, Taiyuan University of Technology, Taiyuan 030024, China

ABSTRACT: Organic surface modification may be critical to the practical use of silicene, which is a novel two-dimensional layered material. It is intriguing to know if organic surface modification seriously impacts the structural, electronic and optical properties of silicene. In this work, we focus on four hydrogenation-based organic surface modification schemes (hydrosilylation, alkoxylation, aminization and phenylation) with the experimentally demonstrated surface coverage of ~ 33%. The geometrical structures, band structures and optical absorption of organically surface-modified silicene have been compared with those of silicene and hydrogenated silicene (H-silicene) in the frame work of density functional theory. It is found that organic surface modification leads to the increase of the buckling distance of silicene, while causing the angles of bonds in the honeycomb structure of silicene to decrease. Although the initial hydrogenation makes silicene become an indirect-bandgap semiconductor, the subsequent organic surface modification schemes further change the band structure of silicene. Hydrosilylation, phenylation, alkoxylation and amination all give rise to the reduction of the bandgap of silicene. Hydrosilylated and phenylated silicene are indirect-bandgap semiconductors, while alkoxylated and aminated silicene are direct-bandgap semiconductors. Changes of the optical absorption induced by organic surface modification are well correlated to the corresponding changes of the band structure.

Keywords: silicene, surface modification, density functional theory, band structure, optical property

[*] Corresponding author E-Mail: xdpi@zju.edu.cn

1. INTRODUCTION

As a novel two-dimensional layered material, silicene owns a series of advantages such as massless Dirac Fermions, quantum Hall effect and compatibility with silicon (Si) technologies.[1-6] It is envisaged that silicene will greatly help Si-based semiconductor industry to produce next-generation devices.[7,8] However, the practical use of silicene is thought to critically depend on its surface modification.[9] Compared with traditional two-dimensional layered materials such as graphene, silicene has a surface with much higher reactivity.[10] The rather reactive surface of silicene should be modified according to targeted applications. It has already been proposed that inorganic surface modification that takes advantage of H, F, O, B, N, P and various metal elements may effectively tune the band structure of silicene, rendering controllable electronic and optical properties of silicene.[11-22] As far as the organic surface modification of silicene is concerned, Rubio-Pereda and Takeuchi have recently demonstrated its possibility theoretically.[10] Nakano et al. even argued that they experimentally obtained organically surface-modified silicene.[23-25] Given the vulnerability of silicene to oxidation, organic surface modification should be a desired means to stabilize silicene, similar to what happens to conventional Si materials.[26-30] Although it has been indicated that organic surface modification may also change the electronic and optical properties of silicene,[23-25] the related theoretical understanding remains elusive.

In this work, we investigate four surface modification schemes (hydrosilylation, phenylation, alkoxylation and aminization) that are based on the hydrogenation of silicene by means of density functional theory (DFT). The specific organic surface coverage of ~ 33% that has been experimentally demonstrated is focused on. Insights on the effects of organic surface modification on the geometrical structure, band structure and optical absorption of silicene are obtained. It is found that organic surface modification leads to the increase of the buckling distance of silicene, while causing the angles of bonds in the honeycomb structure of silicene to decrease. Hydrogenation changes silicene from a semimetal to an indirect-bandgap semiconductor. Subsequent organic surface modification schemes further change the band structure of silicene. Hydrosilylated and phenylated silicene are indirect-bandgap semiconductors, while alkoxylated and aminated silicene are direct-bandgap semiconductors. Hydrosilylation, phenylation, alkoxylation and amination all cause the bandgap of silicene to decrease. The optical absorption of all the organically surface–modified silicene has been discussed.

2. MODEL AND METHOD

Fig. 1 (a) shows the optimized structure of silicene with a top or side view. A 3 × 3 supercell has been adopted to sufficiently optimize the structure of silicene. The distance between adjacent atomic layers is set as 20 Å to avoid image-image interaction. Since organic surface modification is usually carried out at hydrogen-passivated Si surface,[27, 29, 30] silicene is initially hydrogenated. The hydrogenated silicene (H-silicene) is shown in Fig. 1 (b) with a top or side view. We have adopted the most energetically favorable chair-like configuration for

H-silicene.[15] Propylene (CH_2=CH-CH_3), ethyl (CH_3-CH_2-OH), ethylamine (CH_3-CH_2-NH_2) and phenylmagnesium bromide (C_6H_5-MgBr) are representatively chosen for the simulation of hydrosilylation, alkoxylation, aminization and phenylation of silicene, respectively. The resulting organically surface-modified

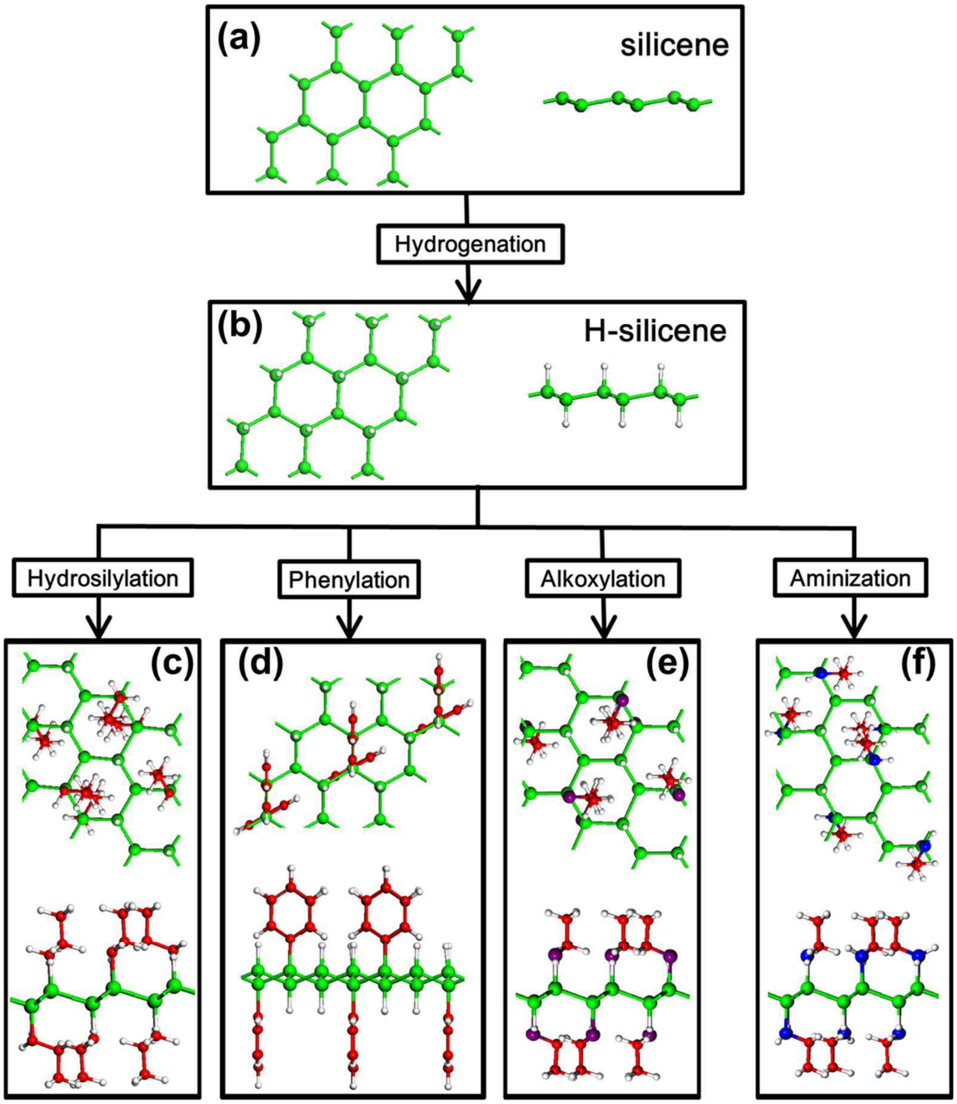

Fig. 1 Optimized structures of (a) silicene, (b) H-silicene, (c) hydrosilylated silicene, (d) phenylated silicene, (e) alkoxylated silicene and (f) aminated silicene. Both top and side views of

each optimized structure are shown. Si, H, C, O and N atoms are denoted by green, white, red, purple and blue balls, respectively.

silicene structures are shown in Fig. 1 (c)-(f) with both top views and side views. In each organically surface-modified silicene structure, the ratio of the number of Si-H bonds to that of Si-X bonds (X=C for hydrosilylation, O for alkoxylation, N for amination and Ph for phenylation) is 2:1, which is consistent with the experimentally observed organic surface coverage of ~ 33%.[25]

The DFT calculations in this work have been performed in the Vienna *ab initio* simulation package (VASP) with the projector-augmented wave (PAW) method.[31,32] The Perdew-Burke-Ernzerhof (PBE) correlation exchange functional at the generalized gradient approximation (GGA) level is adopted. Each structure is optimized to obtain minimized total energy and atomic forces. The Brillouin zone is sampled with a (5×5×1) or (9×9×1) Monkhorst-Pack k-point grid in structural relaxation or density-of-states (DOS) calculations.[33] During the calculation of band structures, 30 points between two neighboring high symmetric k-points are employed. All the calculations are carried out until the change in energy and the force on each atom are less than 1×10^{-6} eV per cell and 1×10^{-5} eV/Å, respectively. It should be noted that DFT calculations usually underestimate the bandgaps of semiconductors because of quasiparticle and excitonic effects.[17,34] However, the relative order for the bandgaps is not affected by the underestimation.[34]

Optical absorption in the direction parallel to the two-dimensional plane is derived from the frequency (ω)-dependent dielectric function ($\varepsilon(\omega)$) of silicene, H-silicene or organically surface-modified silicene in the same direction. The value of $\varepsilon(\omega)$ is first calculated by density functional perturbation theory as implemented in VASP. The imaginary part of $\varepsilon(\omega)$ ($Im\varepsilon(\omega)$) is calculated by summing over the empty conduction band states by using:[35]

$$\mathrm{Im}\varepsilon_{\alpha\beta}(\omega)=\frac{4\pi^2e^2}{\Omega}\lim_{q\to 0}\frac{1}{q^2}\sum\nolimits_{f,i,\mathbf{k}}2w_k\,\delta(\varepsilon_{f\mathbf{k}}-\varepsilon_{i\mathbf{k}}-\omega)\times\langle u_{f\mathbf{k}}+e_{\alpha q}|u_{i\mathbf{k}}\rangle\langle u_{f\mathbf{k}}+e_{\beta q}|u_{i\mathbf{k}}\rangle^{*}, \quad (1)$$

where the index α or β is one Cartesian component of the 3×3 Cartesian tensor; i or f is the initial or final electron transition state; Ω is the volume of the primitive cell; $u_{i\mathbf{k}}$ or $u_{f\mathbf{k}}$ is the cell's periodic part of the orbitals at the k-point of the initial or final electron transition state; e is the unit vector of the Cartesian directions.

The absorption coefficient (A (ω)) is then obtained by using:[36]

$$A(\omega)=\frac{\omega}{C}L\times Im\varepsilon(\omega) \quad , \quad (2)$$

where C is the speed of light, L is the distance between adjacent atomic layers, $Im\varepsilon(\omega)$ is the imaginary part of the dielectric function. It should be noted that the electron-hole excitonic effect is not included during the calculation because of the single-particle approximation in DFT.[31,32] The optical absorption of silicene, H-silicene or organically surface-modified silicene in the direction perpendicular to the two-dimensional plane is dominated by the excitonic absorption, while the optical absorption parallel to the two-dimensional plane is not affected by the excitonic effect.[36]

3. RESULTS AND DISCUSSION

We have obtained the formation energy (E_f) of organically surface-modified silicene by using

$$E_f = E_0 - E_{H-silicene} - \frac{n_H}{2} E_{H_2} - \frac{n_Y}{2} E_{Y_2} - n_C E_C \quad , \tag{3}$$

where $E_{H\text{-}silicene}$ and E_0 are the total energies of H-silicene and organically surface-modified silicene at 0 K, respectively. n_H, n_C and n_Y are the numbers of H, C and Y (Y=O or N) atoms in the ligands attached to H-silicene, respectively. E_{H_2}, E_C and E_{Y_2} are used for the chemical potentials of H, C and O/N, respectively. They are the total energies of hydrogen gas, the total energy per atom of diamond and the total energy of oxygen gas (nitrogen gas) at 0 K, respectively. The values of E_f for organically surface-modified silicene are tabulated in Table 1. It is seen that the values of E_f for hydrosilylated, alkoxylated and aminated silicene are negative, indicating that the hydrosilylation, alkoxylation and amination of H-silicene are exothermic. In contrast, the phenylation of H-silicene is endothermic because E_f is positive for phenylated silicene. Please note that E_f critically depends on the chemical potentials of H, C, O/N. The value of E_f for phenylated silicene may become negative as the chemical potentials of H and C vary.

The binding energy per atom (E_b) of each organically surface-modified silicene structure is calculated by using

$$E_b = \frac{n_{Si}E_{Si} + n_H E_H + n_C E_c^{'} + n_Y E_Y - E_0}{n_{Si} + n_H + n_C + n_Y} \quad , \qquad (4)$$

where n_{Si} is the number of Si atoms in each organically surface-modified silicene structure. E_{Si}, E_H, $E_c^{'}$ and E_Y are the total energy of Si, H, C and Y (Y= O or N) atoms, respectively. The obtained values of E_b are shown in Table 1. All the values of E_b are between 5.0 and 5.8 eV, indicating that significant energy is needed to decompose organically surface-modified silicene. In other words, all the organically surface-modified silicene structures are thermodynamically stable.

In order to further explore the stability of organically surface-modified silicene, we have performed molecular dynamics (MD) simulations on these structures at temperatures of 300 and 600 K. The MD simulations are carried out with the NPT ensemble in the Forcite dynamic calculation scheme. The duration of 2000 ps and the time step of 1 fs are used in the MD simulations. Taking hydrosilylated silicene as an example, at 300 K Si-Si, Si-C, C-C/Si-H and C-H bond-oscillations are 2.1 - 2.4 Å, 1.8 - 2.0 Å, 1.3 - 1.6 Å and 1.0 - 1.2 Å, respectively. The bond-oscillation increases with the increase of temperature from 300 to 600 K (Fig. S1 in the Supporting Information). However, the structure of hydrosilylated silicene basically remains even when the temperature is as high as 600 K. (Fig. S2 in the Supporting Information). What happens to other organically surface-modified silicene is quite similar to the case of hydrosilylated silicene (Figs. S1 and S2 in the Supporting Information). Therefore, we state that the structures of organically surface-modified silicene are pretty stable.

The structural parameters of silicene, H-silicene and organically surface-modified silicene are listed in Table 1. The bond length, bond angle and buckling distance of silicene are originally ~ 2.3 Å, 116.0-116.5° and 0.5 Å, respectively. After hydrogenation, the bond length of Si-Si slightly increases to 2.4 Å. The bond angle of

Table 1. Formulas, structural properties, binding energies (E_b), formation energies (E_f) and bandgap energies (E_g) of silicene, H-silicene and organically surface-modified silicene. The structural properties include the buckling distance (Δ) of Si, the bond length of Si-Si (<Si-Si>), the bond length of Si-X (<Si-X>, X = C for hydrosilylation, O for alkoxylation, N for amination and Ph for phenylation) and the bond angle of Si-Si-Si (∠(Si-Si-Si)).

	Formula	**Δ (Å)**	**<Si-Si> (Å)**	**∠ (Si-Si-Si) (°)**	**<Si-X> (Å)**	**E_b (eV)**	**E_f (eV)**	**E_g (eV)**
Silicene	Si_{18}	0.5	2.3	116.0-116.5	--	--	--	0
H-Silicene	$Si_{18}H_{18}$	0.7	2.4	110.5	1.5	--	--	2.2^i
Hydrosilylated silicene	$Si_{18}C_{18}H_{54}$	0.8	2.3	109.3-113.4	1.9	5.0	-35.4	1.8^i
Phenylated silicene	$Si_{18}C_{36}H_{42}$	0.8	2.3	109.4-109.7	1.9	5.8	10.7	2.0^i
Alkoxylated silicene	$Si_{18}C_{12}O_6H_{42}$	0.8	2.3-2.4	106.4-113.4	1.9	5.0	-26.4	1.7^d
Aminated silicene	$Si_{18}C_{12}N_6H_{48}$	0.8	2.3-2.4	105.8-111.9	1.9	5.1	-25.3	1.7^d

^{i} indirect bandgap. ^{d} direct bandgap.

Si-Si-Si decreases to 110.5°. The buckling distance increases to 0.7 Å. These changes indicate the transition from mixed sp^2/sp^3 hybridization to sp^3 hybridization for Si atoms. Please note that the current structures of silicene and H-silicene are both consistent with those reported in previous works.[14-15, 37-39] After organic surface modification, the further changes in the Si-Si bond length are rather small (< 5%).

However, the buckling distance further increases to 0.8 Å. It is interesting that hydrosilylation, alkoxylation and amination makes the Si-Si-Si bond angle fluctuate in a relatively large range (up to 7°), while phenylation causes the Si-Si-Si bond angle to stabilize at a very small range (109.4-109.7°). It is clear that all the Si-Si-Si bond angles in organically surface-modified silicene are smaller than those in the original silicene (Table 1). In addition, we find that the Si-X bond length is always ~ 1.9 Å no matter what type of organic surface modification is carried out, being larger than the Si-H bond length (1.5 Å).

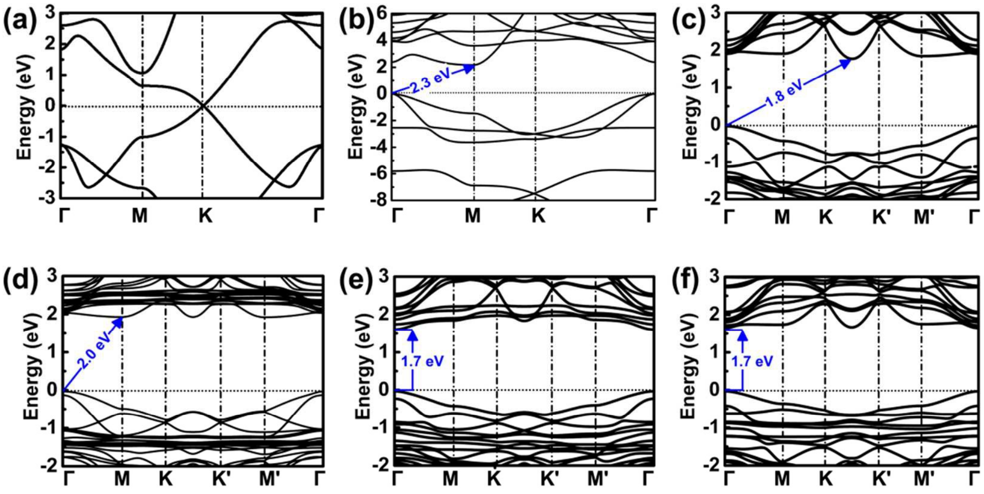

Fig. 2 Band structures of (a) silicene, (b) H-silicene, (c) hydrosilylated silicene, (d) phenylated silicene, (e) alkoxylated silicene and (f) aminated silicene. Energy is shifted so that the Fermi level is at 0 eV.

We now focus on the effect of organic surface modification on the electronic properties of silicene. Fig. 2 (a) shows that silicene is originally a semimetal with the Fermi level crossing both the valence-band maximum and conduction–band minimum. As shown in Fig. 2 (b), H-silicene is an indirect-bandgap semiconductor.

The valence-band maximum appears at the Γ point, while the conduction band minimum appears at the M point. The indirect bandgap is 2.2 eV. Fig. 3 shows the partial DOS (PDOS) of silicene, H-silicene and organically surface-modified silicene. We find that for silicene and H-silicene, the *p*-orbital of Si significantly contributes to the valance band, while the conduction band mainly originates from the *s*-orbital and *p*-orbital of Si (Fig. 3 (a) and (b)). After organic surface modification, the symmetry inside the unit cell of silicene decreases. The K' (M') and K (M) points in the first Brillouin zone are no longer equivalent. Therefore, we have enlarged the first Brillouin zone during the calculation of the band structures of organically surface-modified silicene. For hydrosilylated silicene, the valence-band maximum appears at the Γ point, while the conduction-band minimum appears between the K point and K' point, indicating that hydrosilylated silicene is an indirect-bandgap semiconductor. The indirect bandgap is 1.8 eV (Fig. 2 (c)). The PDOS of hydrosilylated silicene shows that the *p*-orbital of Si, *p*-orbital of C and *s*-orbital of H mainly contribute to the valance band, while the *s*-orbital of Si and *p*-orbital of Si contribute to the conduction band (Fig. 3 (c)). As shown in Fig. 2 (d), the valence-band maximum and conduction-band minimum of the phenylated silicene are located at the Γ point and M point, respectively. The resulting indirect bandgap of phenylated silicene is 2.0 eV. The PDOS analysis indicates the *p*-orbital of C significantly contributed to the valance band and conduction band of phenylated silicene (Fig. 3 (d)). The valence-band maximum and conduction-band minimum are

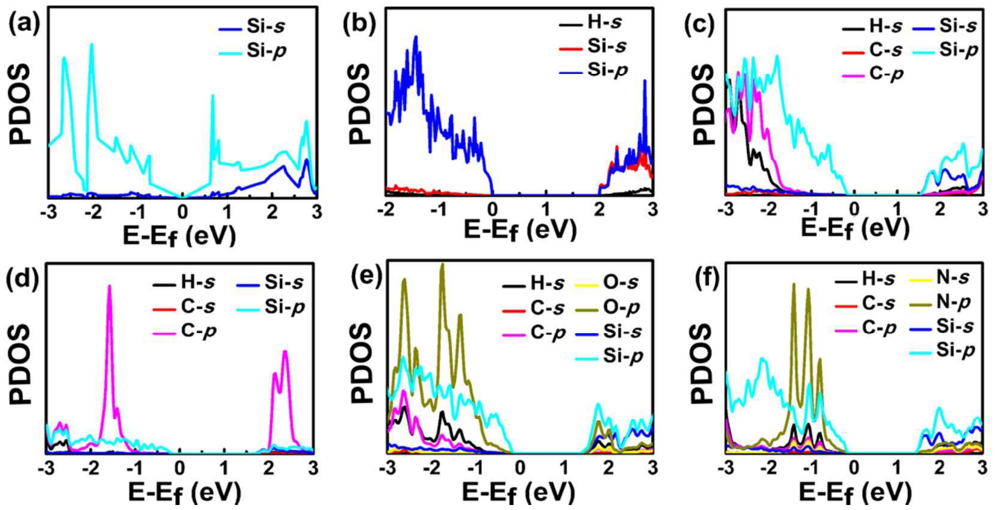

Fig. 3 The partial density of states (PDOS) of (a) silicene, (b) H-silicene, (c) hydrosilylated silicene, (d) phenylated silicene, (e) alkoxylated silicene and (f) aminated silicene. Energy is shifted so that the Fermi level is at 0 eV.

both located at the Γ point for either alkoxylated or aminated silicene (Fig. 2 (e) and Fig. 2 (f)). Hence, both alkoxylated and aminated silicene are direct-bandgap semiconductors. Their direct bandgaps are both ~ 1.7 eV. For alkoxylated (aminated) silicene, the valance band mainly originates from the *p*-orbital of Si and the *p*-orbital of O (N), while the conduction band mainly originates from the *p*-orbital of Si (Fig. 3 (e) and Fig. 3 (f)). The values of the electronegativity of Si, O and N are 1.98, 3.44 and 3.04, respectively. It is well-known that the valance bands are mainly derived

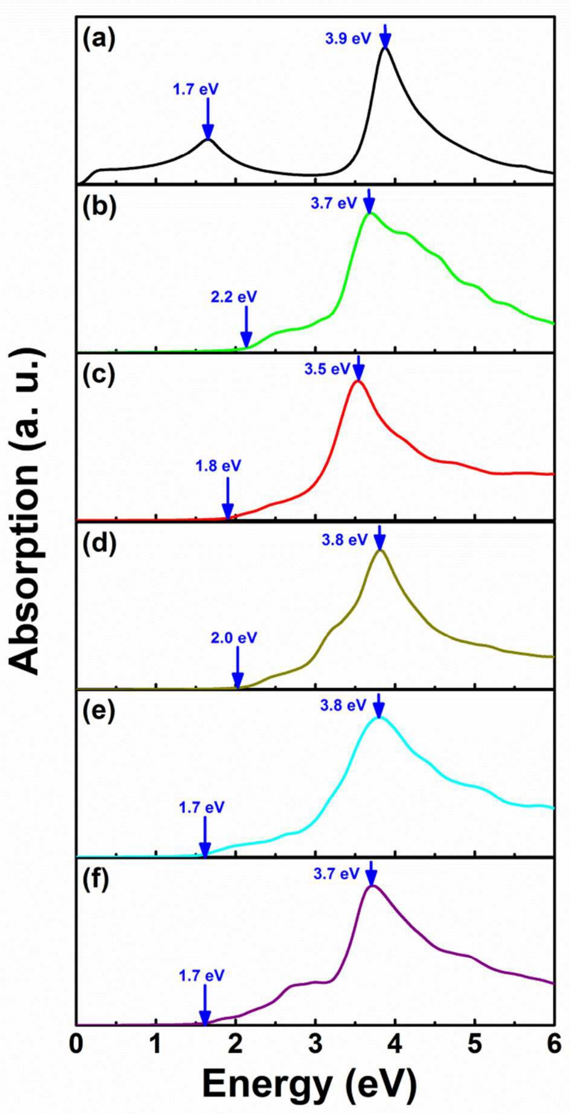

Fig. 4 Optical absorption spectra of (a) silicene, (b) H-silicene, (c) hydrosilylated silicene, (d) phenylated silicene, (e) alkoxylated silicene and (f) aminated silicene.

from the bonding states of atoms with large electronegativity, while the conduction bands are mainly derived from the anti-bonding states of atoms with small electronegativity. Therefore, it is reasonable that the *p*-orbital of O (N) dominates the valance band of alkoxylated (aminated) silicene, while the *p*-orbital of Si dominates the conduction band of alkoxylated (aminated) silicene.

We have also studied the optical absorption of silicene, H-silicene and organically surface-modified silicene, as shown in Fig. 4. For silicene, the zero-bandgap characteristic causes its absorption onset to be located very closely to 0 eV (Fig. 4 (a)). The absorption peaks at 1.7 and 3.9 eV are related to the interband transitions of electrons at the M point ($T_0 \rightarrow T_1$) and Γ point ($T_2 \rightarrow T_3$), respectively. Fig. 5 (a) schematically shows these interband transitions. For H-silicene, the absorption onset is at ~ 2.2 eV (Fig. 4 (b)), which corresponds to the transition of an electron from the valence-band maximum at the Γ point to the conduction-band minimum at the M point ($T_0 \rightarrow T_2$) (Fig. 5 (b)). The prominent absorption peak at 3.7 eV (Fig. 4 (b)) results from the direct transition of an electron at the M point ($T_1 \rightarrow T_2$), as indicated in Fig. 5 (b)). Compared with hydrogenation, hydrosilylation, phenylation, alkoxylation and amination redshift the absorption onset by 0.4, 0.2, 0.5 and 0.5 eV, respectively (Fig. 4 (c)-(f)). After organic surface modification, the shift of the prominent absorption peak is relatively small (in the range from 3.5 to 3.8 eV). The electron transitions of $T_0 \rightarrow T_1$ and $T_2 \rightarrow T_3$ are responsible for the initial and prominent absorption of all the organically surface-modified silicene, respectively (Fig. 5 (c)-(f)). We would like to mention that the true absorption should blueshift for both H-silicene and organically surface-modified silicene because of the underestimation of the transition energy for semiconductors in the current DFT calculation.

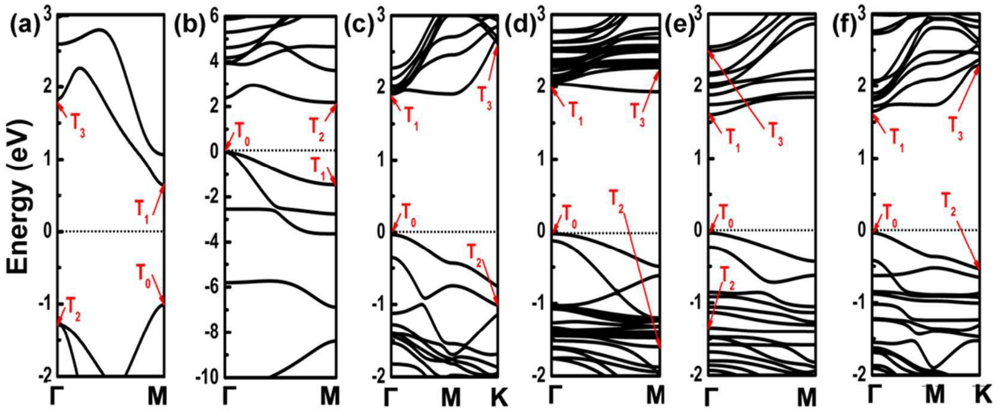

Fig. 5 Part of band structures of (a) silicene, (b) H-silicene, (c) hydrosilylated silicene, (d) phenylated silicene, (e) alkoxylated silicene and (f) aminated silicene. Energy is shifted so that the Fermi level is at 0 eV. The interband transitions of electrons that are responsible for characteristic absorption are indicated.

We want to stress that the optical absorption presented in this work may be qualitatively compared with experimental results very well. For example, the shapes of the absorption spectra of hydrosilylated and aminated silicene are consistent with those experimentally obtained by Nakano et al.[23, 25] In their experiments, the initial and prominent absorption of hydrosilylated silicene appeared in the energies similar to those for aminated silicene. This is basically consistent with what is shown in Fig. 4. It has been indicated that the absorption onset of phenylated silicene is ~ 3 eV by means of a photocurrent measurement. However, the absorption onset of hydrosilylated silicene is ~ 2.7 eV, as evidenced by a UV-visible absorption measurement. The calculated absorption onset of ~2 eV (1.8 eV) for phenylated (hydrosilylated) silicene is within the range underestimated by the current DFT calculation. Therefore, we can state that our calculation can fairly predict the organic surface modification induced relative change in the optical absorption of silicene. We would like to point out that organically surface-modified silicene investigated in this work in fact only absorbs high-energy photons. This disables the use of all the current organically surface-modified silicene to realize the broadband absorption of sunlight in some applications such as photovoltaics. However, the organically surface-modified silicene may hold potential for optoelectronic applications in the UV region (e. g., UV detectors).

We would like to mention that we have also studied the effect of organic surface coverage on the properties of organically surface-modified silicene. It is found that the organic surface coverage actually makes a difference for all the surface modification schemes. For example, when the coverage of propylene-derived ligands changes from 5% to 11%, 33% and 44%, the bandgap of propylene-hydrosilylated silicene varies in the range from 1.6 to 1.9 eV with an either direct-bandgap or indirect-bandgap nature (Fig. S3 in the Supporting Information). This indicates that the surface coverage is an added means to tune the electronic and optical properties of organically surface-modified silicene.

4. CONCLUSIONS

We have investigated surface-modified silicene with an organic surface coverage of ~ 33% that is obtained by the hydrosilylation, alkoxylation, aminization or phenylation of hydrogenated silicene. It is found that organic surface modification increases the buckling distance of silicene, while decreasing the angles of bonds in the honeycomb structure of silicene. The initial hydrogenation changes silicene from a semimetal to an indirect-bandgap semiconductor. Subsequent hydrosilylation, alkoxylation, aminization and phenylation all further change the band structure of silicene. Hydrosilylated and phenylated silicene are indirect-bandgap semiconductors. In contrast, alkoxylated and aminated silicene are direct-bandgap semiconductors. The bandgap of silicene is reduced by all the organic surface modification. The changes of the band structure of silicene give rise to corresponding changes of the optical absorption of silicene. We have finally indicated that the properties of organically surface-modified silicene may actually change with the organic surface coverage.

ACKNOWLEDGEMENTS

We thank Prof. Guy Le Lay at Aix-Marseille University for insightful discussion. Shanghai Supercomputer Center is acknowledged for providing computation resources. This work is mainly supported by the 973 program (Grant No. 2013CB632101) and the NSFC for excellent young researchers (Grant No. 61222404). Partial support is provided by the Fundamental Research Funds for the Central Universities (2014XZZX003-09).

REFERENCES

(1) L. Chen, C. C. Liu, B. Feng, X. He, P. Cheng, Z. Ding, S. Meng, Y. Yao and K. Wu, *Phys. Rev. Lett.*, 2012, **109**, 056804.

(2) L. Meng, Y. Wang, L. Zhang, S. Du, R. Wu, L. Li, Y. Zhang, G. Li, H. Zhou, W. Hofer and H. Gao, *Nano Lett.*, 2013, **13**, 685-690.

(3) C. C. Liu, W. Feng and Y. Yao, *Phys. Rev. Lett.*, 2011, **107**, 076802.

(4) P. De Padova, C. Quaresima, C. Ottaviani, P. Sheverdyaeva, P. Moras, C. Carbone, D. Topwal, B. Olivieri, A. Kara, H. Oughaddou, A. Bernard and G. Le Lay, *Appl. Phys. Lett.*, 2010, **96**, 261905.

(5) P. Vogt, P. De Padova, C. Quaresima, J. Avila, E. Frantzeskakis, M. C. Asensio, A. Resta, B. Ealet and G. Le Lay, *Phys. Rev. Lett.*, 2012, **108**, 155501.

(6) M. Ezawa, *Phys. Rev. Lett.*, 2012, **109**, 055502.

(7) K. J. Koski and Y. Cui, *ACS Nano*, 2013, **7**, 3739-3743.

(8) A. Kara, H. Enriquez, A. P. Seitsonen, L. C. Lew Yan Voo n, S. Vizzini, B. Aufray and H. Oughaddou, *Surf. Sci. Rep.*, 2012, **67**, 1-18.

(9) M. Xu, T. Liang, M. Shi and H. Chen, *Chem. Rev.*, 2013, **113**, 3766-3798.

(10) P. Rubio-Pereda and N. Takeuchi, *J. Chem. Phys.*, 2013, **138**, 194702.

(11) H. Sahin and F. M. Peeters, *Phys. Rev. B*, 2013, **87**, 085423.

(12) J. Sivek, H. Sahin, B. Partoens and F. M. Peeters, *Phys. Rev. B*, 2013, **87**, 085444.

(13) B. Huang, H. J. Xiang and S. Wei, *Phys. Rev. Lett.*, 2013, **111**, 145502.

(14) M. Houssa, E. Scalise, K. Sankaran, G. Pourtois and V. V. Afanas'ev, *Appl. Phys. Lett.*, 2011, **98**, 223107.

(15) Y. Ding and Y. Wang, *Appl. Phys. Lett.*, 2012, **100**, 083102.

(16) N. Gao, W. T. Zheng and Q. Jiang, *Phys. Chem. Chem. Phys.*, 2012, **14**, 257-261.

(17) R. Wang, X. D. Pi, Z. Ni, Y. Liu, S. Lin, M. Xu and D. Yang, *Sci. Rep.*, 2013, **3**, 3507.

(18) F. Zheng, C. Zhang, S. Yan and F. Li, *J. Mater. Chem. C*, 2013, **1**, 2735-2743.

(19) R. Quhe, R. Fei, Q. Liu, J. Zheng, H. Li, C. Xu, Z. Ni, Y. Wang, D. Yu, Z. Gao and J. Lu, *Sci. Rep.*, 2012, **2**, 853.

(20) J. Dai, Y. Zhao, X. Wu, J. Yang and X. Zeng, *J. Phys. Chem. Lett.*, 2013, **4**, 561-567.

(21) X. D. Pi, Z. Ni, Y. Liu, Z. Ruan, M. Xu and D. Yang, *Phys. Chem. Chem. Phys*, 2015, **17**, 4146-4151.

(22) H. Liu, N. Han and J. Zhao, *J. Phys. Condens. Mat.*, 2014, **26**, 475303.

(23) H. Nakano, M. Nakano, K. Nakanishi, D. Tanaka, Y. Sugiyama, T. Ikuno, H. Okamoto and T. Ohta, *J. Am. Chem. Soc.*, 2012, **134**, 5452-5455.

(24) H. Okamoto, Y. Kumai, Y. Sugiyama, T. Mitsuoka, K. Nakanishi, T. Ohta, H. Nozaki, S. Yamaguchi, S. Shirai and H. Nakano, *J. Am. Chem. Soc.*, 2010, **132**, 2710-2718.

(25) Y. Sugiyama, H. Okamoto, T. Mitsuoka, T. Morikawa, K. Nakanishi, T. Ohta and H. Nakano *J. Am. Chem. Soc.*, 2010, **132**, 5946-5947.

(26) M. Linford and C. Chidsey, *J. Am. Chem. Soc.*, 1993, **115**, 12631-12632.

(27) J. G. C. Veinot, *Chem. Commun.*, 2006, 4160-4168.

(28) X. D. Pi, R. Wang and D. Yang, *J. Mater. Sci. & Tech.*, 2014, **30**, 639-643.

(29) J. Buriak, *Chem. Rev.*, 2002, **102**, 1271-1308.

(30) R. Wang, X. D. Pi and D. Yang, *J. Phys. Chem. C*, 2012, **116**, 5401-5406.

(31) P. E. Blöchl, *Phys. Rev. B*, 1994, **50**, 17953-17979.

(32) G. Kresse and D. Joubert, *Phys. Rev. B*, 1999, **59**, 1758-1775.

(33) H. J. Monkhorst and J. D. Pack, *Phys. Rev. B*, 1976, **13**, 5188-5192.

(34) A. J. Williamson, J. C. Grossman, R. Q. Hood, A. Puzder and G. Galli, *Phys. Rev. Lett.*, 2002, **89**, 196803.

(35) M. Gajdoš, K. Hummer, G. Kresse, J. Furthmüller and F. Bechstedt, Phys. Rev. B: Condens. Matter Mater. Phys., 2006, **73**, 045112.

(36) L. Matthes, P. Gori, O. Pulci and F. Bechstedt, *Phys. Rev. B*, 2013, **87**, 035438.

(37) S. Cahangirov, M. Topsakal, E. Aktürk, H. Şahin and S. Ciraci, *Phys. Rev. Lett.*, 2009, **102**, 236804.

(38) M. Houssa, G. Pourtois, V. V. Afanas’ev and A. Stesmans, *Appl. Phys. Lett.*, 2010, **97**, 112106.

(39) L. C. Lew Yan Voon, E. Sandberg, R. S. Aga and A. A. Farajian, *Appl. Phys. Lett.*, 2010, **97**, 163114.